Science of Advanced Materials
Vol. 4, 1–13, 2012

Recent Progresses in Improving Nanowire Photodetector Performances

Chaoyi Yan and Pooi See Lee*

School of Materials Science and Engineering, Nanyang Technological University, Singapore 639798

Recent advancements of nanowire (NW) photodetector performances are reviewed. This review focuses on the key performance improvements and strategies towards low-cost device fabrication, fast photoresponse time, high wavelength selectivity and high sensitivity, which are among the most important characteristics of NW photodetectors. Representative reports demonstrating significant improvements in the aforementioned device properties are summarized and analysed. NW networks are emerging as promising structures than conventional single NW devices which are facing NW assembly problem and require expensive and intense lithography steps. The network devices are also advantageous in achieving fast photoresponse time due to the fast response rate of junction barriers. High wavelength selectivity in NW photodetectors was achieved with ternary alloyed NWs with tunable bandgaps and hence cut-off wavelengths. Ternary oxides with larger bandgaps than those common binary oxides were found to be superior candidates for selectively deep-UV detection. Sensitivity can be improved by functionalizing the NW channel with polymer or making use of the piezoelectric property of the NWs. The progresses made in improving photodetector performances are expected to greatly accelerate their practical applications. An outlook and future research directions are also presented.

Keywords: Nanowire, Photodetector, Improvements, High-Performance.

RESEARCH ARTICLE

CONTENTS

1. INTRODUCTION

Photodetector is one of the most important applications of semiconductor nanowires (NWs) and has attracted extensive attentions recently.[1–7] The novel nanostructures with unique properties are expected to be superior building blocks for nanoscale photodetectors than their bulk or thin film counterparts. The high surface-to-volume ratio and unique one-dimensionality of NWs are highly desirable characteristics for the fabrication of high-performance photodetectors. Future research in NW photodetectors towards practical applications aims to achieve low-fabrication cost, fast photoresponse time, high wavelength selectivity, high sensitivity, high stability, excellent performance consistency, etc. Significant progresses have been made recently towards commercialized applications and were summarized in several excellent reviews previously.[3, 8, 9]

In this review, we first give a brief summary of the nanomaterials investigated for photodetector applications to date. Then we present the recent progresses in NW photodetectors in the following 4 aspects: (1) low-cost device fabrication, (2) fast photoresponse time, (3) high wavelength selectivity and (4) high sensitivity. Our review focuses on the development of photodetector design and performance improvements in these 4 categories and is different from the previous review articles, which mainly focused on the types of NW materials[3] or types of device configurations.[9] We first summarized the recent progresses towards low-cost device fabrication, which is a crucial determining factor for potential large scale industrial application. Interestingly, it has been evidential that NW networks were found to be promising alternative solutions than individual NW for the fabrication of low-cost

*Author to whom correspondence should be addressed.

photodetectors with superior performances.[10–12] Subsequently, progresses towards fast photoresponse time are presented, with special focus on NW network devices[10, 11] and Schottky-type photodetectors.[13] Progresses towards high wavelength selectivity include research in ternary wide bandgap oxides[14] and ternary alloyed materials[15] will be highlighted. Polymer surface functionalization[5] and utilization of piezo-phototronic effects[1] were recently demonstrated to be efficient methods to enhance the photodetector sensitivity. Finally, this review ends with conclusion and a panoramic outlook. The present review article outlines the representative developments on photodetector performances, focusing on the innovative works which may significantly advance photodetector applications.

2. NANOMATERIALS INVESTIGATED

Numerous nanomaterials have been investigated for photodetector applications. Table I summarizes the typical groups of materials investigated in literature for NW photodetector applications. For each type of material, only one representative reference is provided to give a sample view although there are more works on the similar material. Majority of the research works were focusing on inorganic nanomaterials, especially semiconductor NWs (Table I). Some reports on the metal, superconductor and organic NW photodetectors can also be found. Photodetectors based on inorganic semiconductor NWs in particular oxide nanostructures in general are stable, cost-effective and easy to be fabricated considering the well-established synthetic methods for metal oxide NWs. Thus, oxide NW photodetectors have attracted more attention and are considered as superior candidates for potential large-scale production. In this review, representative advancements in the photodetector properties are mainly from oxide NWs devices.

Table I. Groups of nanomaterials investigated for photodetector applications.

Materials	References
Inorganic	
Semiconductor	
Elemental	
IV	Si,[16] Ge[10]
VI	Se,[17] Te[18]
Binary	
Non-oxide	ZnS,[4] ZnSe,[19] ZnTe,[20] CdS,[21] CdSe,[22] CdTe,[22] InP,[23] GaN,[24] Sb_2Se_3,[25] ZrS_2,[26] Ag_2S,[27] InSe,[28] In_2Se_3,[2] Bi_2S_3,[29] Zn_3P_2[30]
Oxide	ZnO,[6] SnO_2,[31] In_2O_3,[32] CdO,[33] V_2O_5,[34] Ga_2O_3,[35] Fe_2O_3,[36] Cu_2O,[37] CeO_2,[38] TiO_2,[39] Sb_2O_3[40]
Ternary	
Alloy	$Zn_xCd_{1-x}Se$,[15] $ZnSe_{1-x}Te_x$,[41] $Cd_{1-x}Zn_xS$[42]
Oxide	Zn_2GeO_4,[11] $In_2Ge_2O_7$,[14] $ZnSnO_3$,[43] $ZnGa_2O_4$[44]
Metal	Au[45]
Superconductor	NbN[46]
Organic	F8T2,[47] MeSq,[48] C_{60}[49]
Hybrid	
Inorganic/inorganic	Au/SiO_2,[50] Au/Ga_2O_3,[51] ZnO/Si,[52] ZnS/InP,[53] Ge/CdS,[54] ZnO/GaN,[55] Ag/Ni,[56] RuO_2/TiO_2,[57] Ga/ZnS,[58] $ZnSe/SiO_2$,[59] Au/CdSe/Au[60]
Organic/inorganic	Si/porphyrin,[61] CdS/PPY,[62] ZnS/CNT[63]

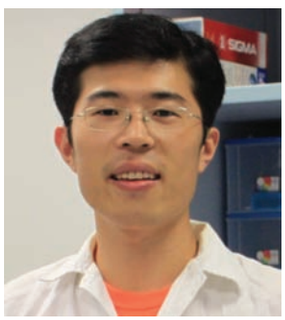

RESEARCH ARTICLE

3. PROGRESSES IN NANOWIRE PHOTODETECTOR PERFORMANCES

3.1. Low-Cost Device Fabrication Processes for Emerging Network Devices

Extensive reports can be found on NW photodetectors, with most of them focusing on single-NW devices. However, the fabrication of single-NW devices requires complex and expensive lithography steps to address the single NW, such as electron beam lithography (EBL), focused ion beam (FIB), etc. The high fabrication cost has severely deterred the industrial applications of NW photodetectors.

Recently, NW networks have attracted much interest as alternative detection channels in photodetectors. The facile and low-cost fabrication processes of network devices allow potential large-scale industrial fabrication of NW photodetectors. A typical assembly method of NW networks and its corresponding device fabrication processes are shown in Figure 1.[64] After growing the Si NWs using conventional chemical vapour deposition (CVD) method, surface functionalization of the SiNWs were carried out (Fig. 1(a)).[64] Surface functionalization is a critical process to obtain stable NW dispersion, without which the suspension solutions began to aggregate even after few hours.[64]

The NW assembly and consequent device fabrication processes can be carried out using simply the conventional micro-fabrication techniques as shown in Figure 1(b). The neutral regions were patterned by PL and covered with methyl-terminated octadecyltrichlorosilane (OTS) SAM,[64] which facilitates hydroxyl groups (−OH) adsorption on SiO_2 surface. Selective and preferential adsorption of the surface functionalized Si NWs with positive surface charge onto the negatively charge regions can be realized and almost nothing were adsorbed on the neutral region due to the lack of electrostatic attraction force. Metal electrodes were patterned on those assembled NW networks simply using conventional low-cost micro-fabrication techniques. Scanning electron microscopy (SEM) images of the assembled NW network devices are shown in Figures 2(a and b), respectively.[64] An optical image of the device arrays is depicted in Figure 2(c) with a detailed view of individual device shown in the inset. Output characteristic

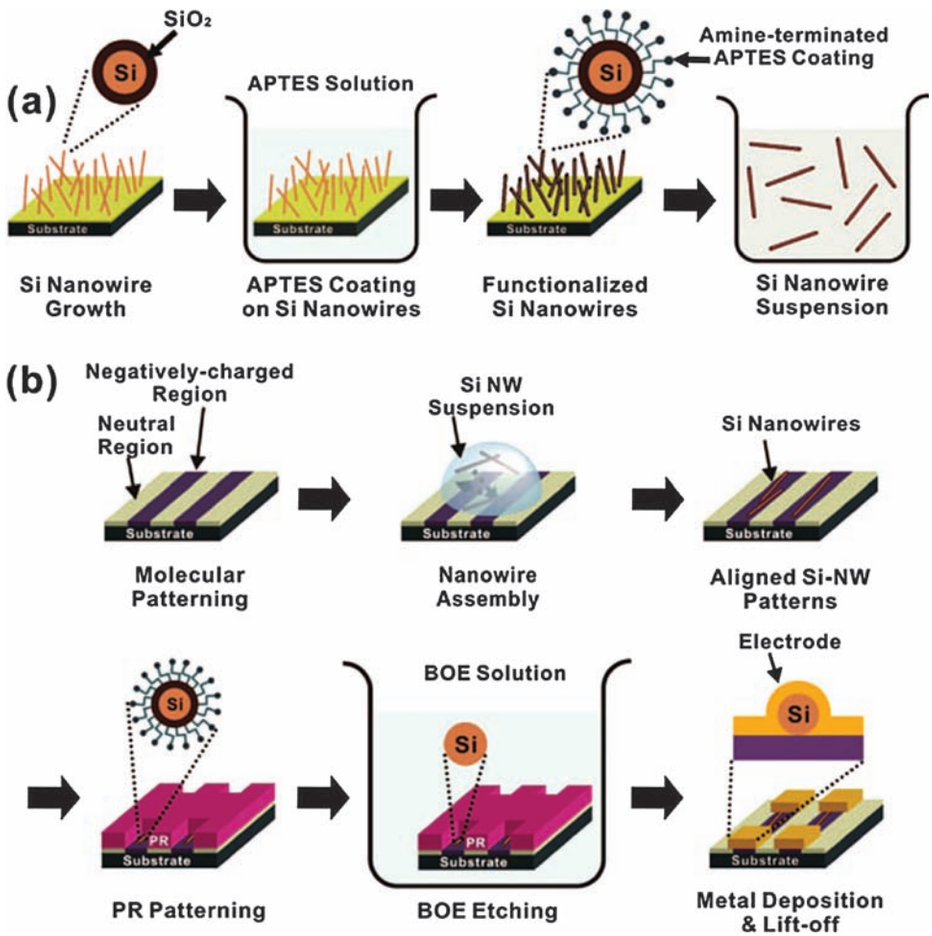

Fig. 1. (a) Schematic diagram of preparing functionalized SiNW suspensions. (b) Schematic diagram for the large-scale NW assembly for nanoelectronic devices. Reprinted with permission from [64], k. Heo et al., *Nano Lett.* 8, 4523 **(2008)**. © 2008, American Chemical Society.

RESEARCH ARTICLE

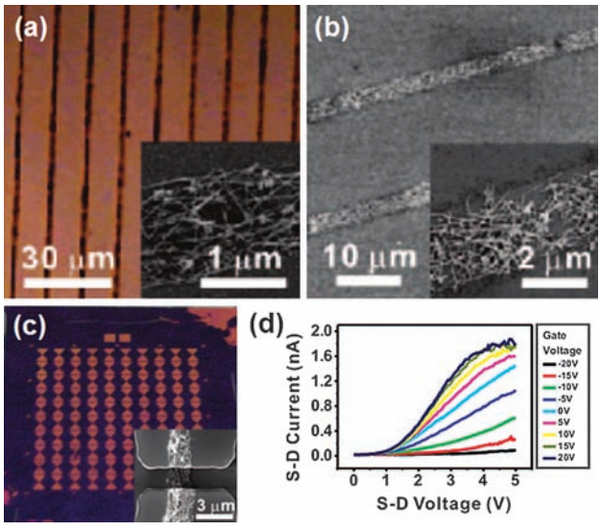

Fig. 2. Optical images of the SiNWs selectively assembled on patterned regions of (a) Au substrates and (b) SiO_2 substrates. (c) Optical image of a device array fabricated only using conventional microelectronic facilities. A typical SEM image of a device is shown in the inset. (d) *I–V* characteristics of a typical device based on *n*-type SiNW networks. Reprinted with permission from [64], k. Heo et al., *Nano Lett.* 8, 4523 **(2008)**. © 2008, American Chemical Society.

from a network device is shown in Figure 2(d).[64] Typical *n*-type semiconducting behaviour can be clearly viewed, as expected for the *n*-type Si NWs. This shows that the entangled NW networks can function as efficiently as previous single NW devices, but allow much lower fabrication cost.

Similar field effect transistors (FETs) using randomly dispersed ZnO NW networks were also reported (Ref. [12]). The fabrication of network devices requires less intense lithography steps compared with single-NW devices and hence requires low fabrication cost. The ZnO NW networks/lawns were generated by a direct stamping process by pressing the donor substrate against the receiver substrate.[12] The receiver substrate was functionalized with poly-L-lysine to enhance adherent force.[65] For a given donor NW density and pressing pressure, the NW density in the networks can be properly controlled via the number of consecutive stamping processes.[12] Typical optical and SEM images of the macro-electronic devices are shown in Figure 3(a).[12] The channel length of the device shown in Figure 3(a) is 20 μm. As can be clearly viewed, the source and drain were not bridged directly by individual NW; instead, the conducting channel was composed of multiple interconnected NWs.[12] Transfer characteristics of such network devices with different channel lengths (5, 15, 20 and 50 μm) are shown in Figure 3(b).[12] Typical *n*-type semiconducting behaviours were observed for all the devices indicating good connectivity for those channel lengths investigated. The variation in ON current is attributed to the increase of nodes in the networks with longer channel lengths and hence increase of the overall resistivity.[12] The authors showed that NW network devices with reliable and consistent performances can be readily fabricated with much lower fabrication cost. Those network devices may serve as promising alternative configurations for single-NW devices for optoelectronic applications, such as photodetectors.

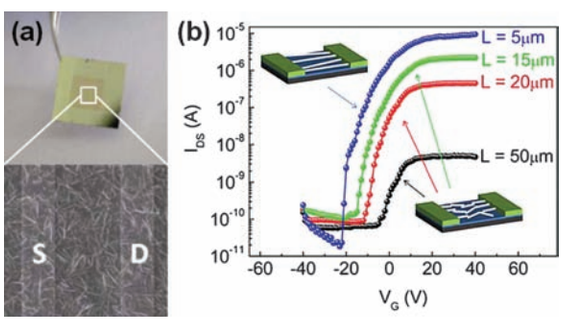

Fig. 3. (a) Optical and SEM image of ZnO NW network devices. The channel length is 20 μm. (b) Transfer characteristics of network transistors with difference channel lengths ($V_{DS} = 4$ V). 5 μm device consist NWs directly bridging the source and drain, while longer channel lengths consist entangled NW networks, as indicated by the insets. Reprinted with permission from [12], H. E. Unalan et al., *Appl. Phys. Lett.* 94, 163501 **(2009)**. © 2009, American Institute of Physics.

Recently, we have reported the comparative studies of NW network and single NW photodetectors attained via facile fabrication processes and detailed its superior performances.[10,11] The schematic illustration of the single NW and NW network photodetectors and the respective photoresponse behaviour are shown in Figure 4.[10] The Ge NW networks were formed by dispersing NW solution on the pre-patterned electrodes. Randomly oriented and entangled Ge NW networks can be observed lying between the electrodes when the solution was dried. Single NW devices were fabricated via similar methods by controlling the NW concentration in solution. Schematic diagrams and *I–V* curves for those single-NW and network devices are shown in Figure 4.[10] Good Ohmic conductance was observed for the single-NW devices while the *I–V* curve for network devices were typically asymmetric due to the different contact points and interfacial conditions at the source/drain electrodes.[10] It should be highlighted that the conducting mechanisms are different for single-NW and network devices. The resistance is dominated by the NW conducting channel itself in the single-NW device with Ohmic contact, however, the resistance is dominated by the NW–NW junctions in the network devices.[10] We suggest that this unique conducting mechanism for network devices are particularly useful for photodetector applications with fast response and reset time (see discussion in the following section).

3.2. Fast Photoresponse Time

Fast response and reset time is one of the highly desirable properties for future high-speed photodetectors, especially

RESEARCH ARTICLE

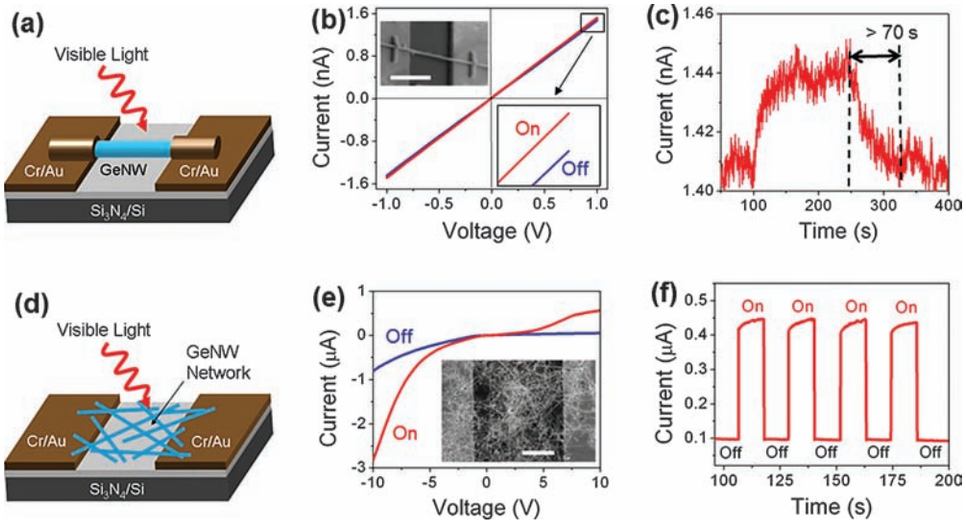

Fig. 4. Schematic models, *I–V* curves and photoresponsive characteristics of (a–c) single Ge NW and (d–f) NW network devices. The scale bars in the insets of (b and e) are 5 μm. Reprinted with permission from [10], C. Y. Yan et al., *ACS Appl. Mater. Interfaces* 2, 1794 **(2010)**. © 2010, American Chemical Society.

for the tracing of light with varying intensity/wavelength. However, conventional photodetectors using single NW detection channels usually gave a response and reset time in the range of tens of second or even up to hours.[6, 7, 13, 66, 67] Designing novel NW photodetector configurations or sensing mechanisms to achieve fast photoresponse time is a crucial requirement for future applications. In this section, we summarize the recent progresses in improving the response and reset time of NW photodetectors.

Fast photoresponse time has been observed in photodetectors using NW networks.[10, 11] The switching behaviour of single Ge NW photodetector and network devices are shown in Figures 4(c and f), respectively. While the reset time (defined as the time require to fully recover to initial value) for single Ge NW photodetector is > 70 s, fast reset time (< 1 s) was observed for network devices (Fig. 4(f) and Fig. 5(a)).[10] The fast response and reset time of network devices enables the efficient tracing of rapidly changed incident light. A typical multi-step switching behaviour of network device is shown in Figure 5(b).[10] The fast photoresponse time in network devices is attributed to the unique junction-dominated conduction mechanism. Unlike single NW photodetector, the resistance of network channel is dominated by the NW–NW junctions (Fig. 5(d)).[10] The conduction and valance bands of Ge would bend upwards at the Ge/GeO_x surface due to the negative charge induced hole accumulation.[68] This band bending would pose as conduction barriers for either electrons or hole transporting through the percolated networks. This NW–NW junction is sensitive to incident light. When the NW is illuminated with light, electron–hole pairs would be generated and holes would be attracted to the surface to fill the negative charge traps, resulting in a lowering of the effective barrier height. Consequently, the conductance of the network would change significantly due to the dominate role of the NW junctions. The reset time for single NW device, which is associated with the surface adsorption and desorption of oxygen molecules, is usually quite slow (> 70 s). The response rate of junction barrier, which can be treated as two back-to-back Schottky barriers, is much faster.[10, 13, 69]

Analogously, fast photoresponse time was also observed in zinc germanate (Zn_2GeO_4, ZGO) NW network photodetectors.[11] Schematic diagrams of the ZGO network devices is shown in Figure 6(a). The network was formed by dispersing ZGO NW solution on the pre-patterned

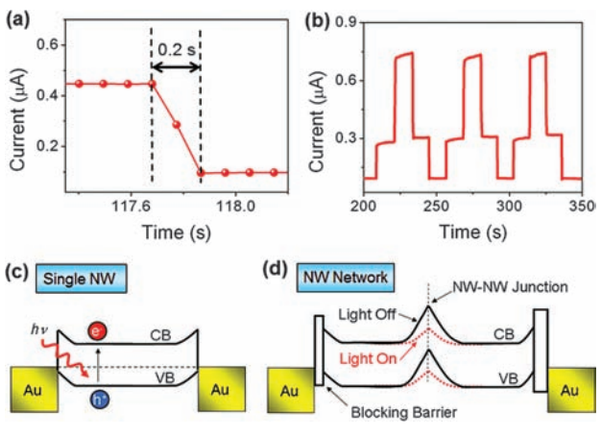

Fig. 5. (a) Detailed view of a current decay process showing the fast reset time. (b) Multiple-step photoresponse characteristics of network devices enabled by the fast response and reset time. (c, d) Schematic illustrations of the band diagrams for single-NW and network devices. Reprinted with permission from [10], C. Y. Yan et al., *ACS Appl. Mater. Interfaces* 2, 1794 **(2010)**. © 2010, American Chemical Society.

RESEARCH ARTICLE

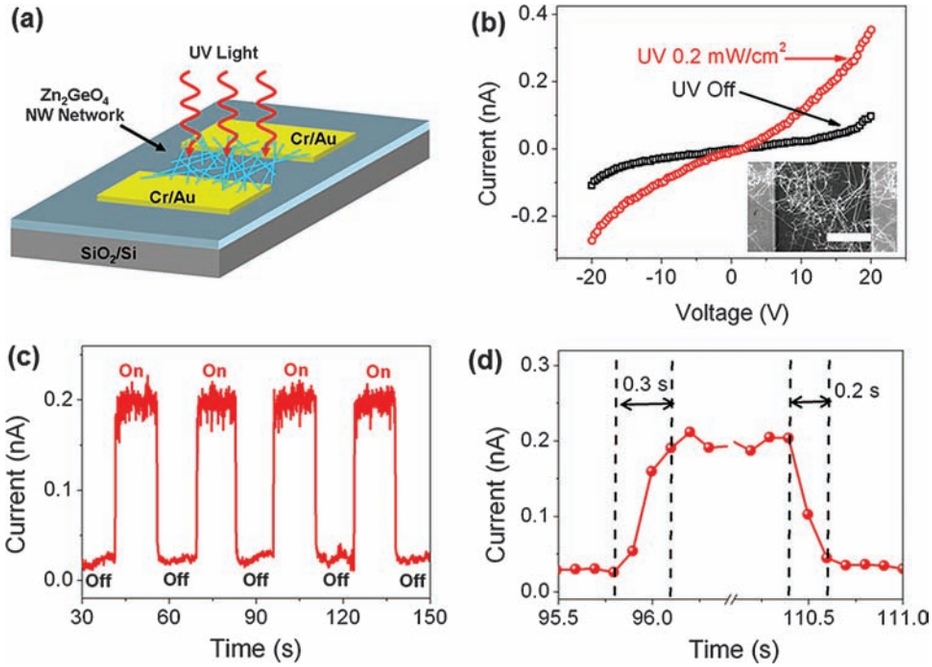

Fig. 6. (a) Schematic model of ZGO NW network photodetectors. (b) *I–V* curves and (c) photoresponsive characteristics of network devices. (d) Enlarged view of current change process showing the fast response and reset time. Reprinted with permission from [11], C. Y. Yan et al., *Appl. Phys. Lett.* 96, 053108 **(2010)**. © 2010, American Institute of Physics.

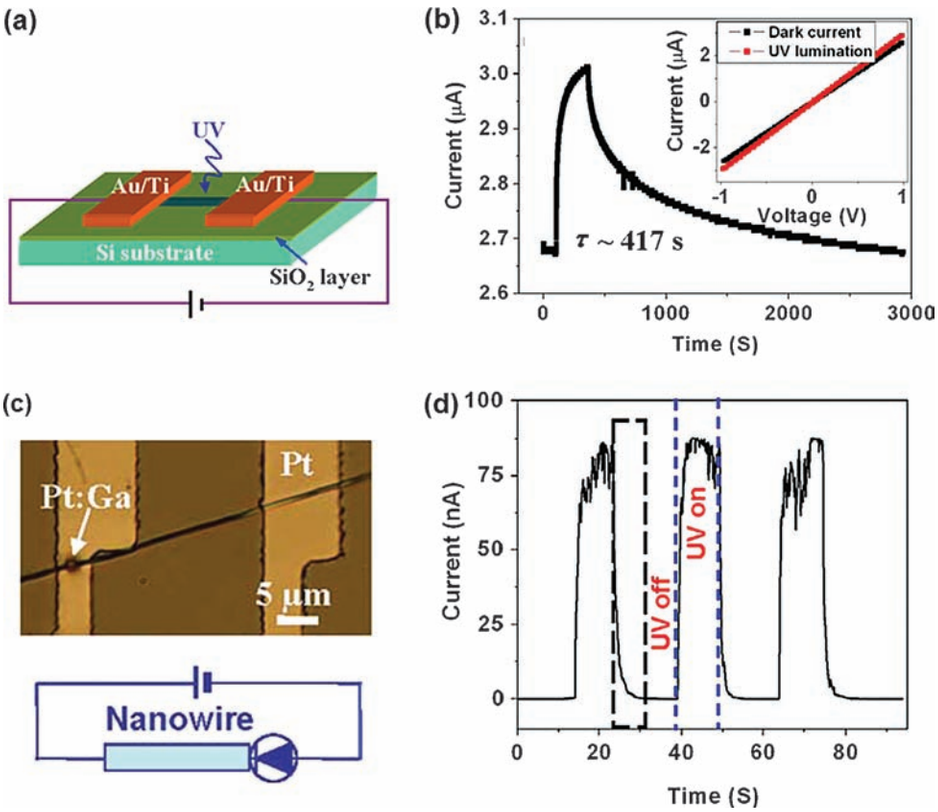

Fig. 7. (a, b) Schematic model and photoresponsive behaviour of ZnO NW photodetectors with Ohmic contact. Inset in (b) is the *I–V* behaviour of the device showing Ohmic conductance. (c, d) Optical image and photoresponsive behaviour of devices with Schottky contact. Reprinted with permission from [13], J. Zhou et al., *Appl. Phys. Lett.* 94, 191103 **(2009)**. © 2009, American Institute of Physics.

RESEARCH ARTICLE

electrodes. Figure 6(b) is a typical *I–V* curve for the network device with (red curve) and without (black curve) 265 nm UV light illumination.[11] Switching behaviour of the device is shown in Figure 6(c), with enhanced view of current increase and decay processes shown in Figure 6(d). Fast response time (0.3 s) and reset time (0.2 s) was observed.[11] Detailed characterizations showed that fast photoresponse time was exclusively observed for all the network devices.[11] The fast photoresponse time was also attributed to the unique junction dominated conductance in the network devices,[11, 70, 71] which is not available in single-NW devices.

Zhou et al. reported the use of Schottky contacts to improve the photoresponse time of ZnO NW photodetectors.[13] Figure 7 shows the comparative studies of ZnO NW devices with Ohmic and Schottky contacts.[13] Analogous to most of the previous reports, ZnO NW photodetector with symmetric electrodes (Au/Ti) showed Ohmic behaviour and a slow photoresponse time, due to the slow processes of oxygen adsorption and desorption.[13] The current cannot recover to its initial value even after ~2500 s (Fig. 7(b)).[13] However, a fast reset time of 0.8 s (in their work defined as the time needed to recover to 1/*e*) was observed in NW device with Schottky contact. The Schottky devices were fabricated as following: Pt microelectrodes were first deposited on SiO_2/Si substrates using photolithography; ZnO NWs were transferred to the substrate via dry scratching; one end of the device was treated using FIB to deposit additional Pt:Ga contact to improve the contact conditions. With the untreated end of poor contact conditions, Schottky conductance was observed for such devices. The fast photoresponse rate was attributed to the intrinsic properties associated with the Schottky barrier. When UV light was turned on, new electron–hole pairs were generated, leading to a rapid increase of the carrier density and hence lowering of the effective barrier height. When UV light was turned off, the carriers would combine and the barrier height would increase rapidly and dramatically. Oxygen is only required to be re-adsorbed to the interfacial Schottky contact region to recover the barrier conditions.[13] As a result, the response and reset time is much faster than the NW device with Ohmic contact, where the resistance is dominated by the NW itself and oxygen need to be re-adsorbed to the whole surface to restore the current value.

Operation of photodetectors with intentionally created Schottky contacts is similar to the network devices, where the switching is also determined by the junction barriers (back-to-back Schottky barriers). Fast photoresponses were observed in both type of devices. However, the fabrication of Schottky contacts for single-NW device requires complex, high-cost and low-yield lithography steps, which may limit their future industrial applications which require cost-effective large scale fabrication.

Polymer functionalization was found to be an efficient way to improve the photoresponse time of NW photodetectors.[13] The current would decay to its initial value within 20 ms for Schottky-type ZnO NW photodetectors functionalized with PDADMAC and PSS polymers (Fig. 8(b) inset).[13] This is much faster than the reset time > 400 s for device with Ohmic contact (Fig. 7(b)) and 0.8 s for device with only Schottky contact (Fig. 7(d)). The underlying mechanisms for the improvement by surface coating is not fully understood yet.[13] It might be possible that the polymer coating affects the response rate of the Schottky barrier and lead to further enhancement in photoresponse rate or the enhancement was due to the interaction of surface coating with NW volume. The authors did not report the effect of surface coating on Ohmic devices, which may shed light on this issue.

Recently, Bando and Golberg group has made significant progresses in the area of NW photodetectors.[2–4, 8, 14, 19, 21, 25, 26, 34, 72, 73] In particular, fast photoresponse time was typical observed in those photodetectors with NW or nanobelt detection channels.[2–4, 8, 14, 19, 21, 25, 26, 34, 72, 73] Figure 9 shows the representative characterizations of In_2Se_3 NW photodetectors.[2] Devices based on single NW were fabricated using EBL (Figs. 9(a and b) inset) and responded to the incident visible light (500 nm).[2]

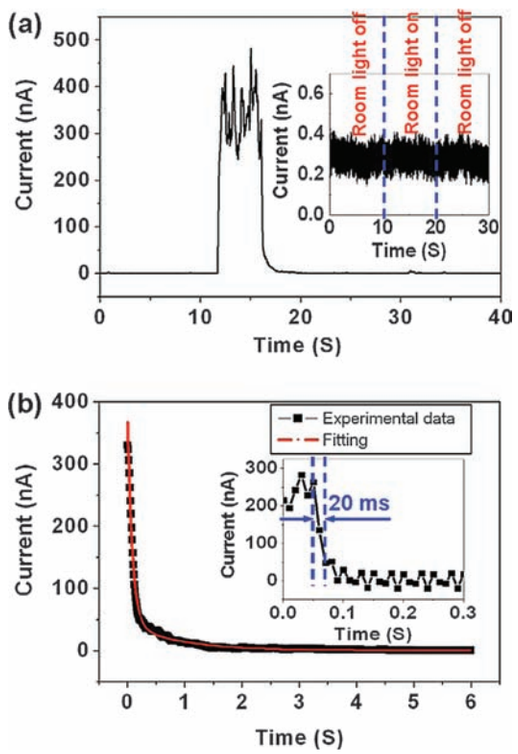

Fig. 8. (a) Photocurrent of a polymer functionalized Schottky-type ZnO NW photodetector. The inset shows the response of the device when room light was turned on and off. (b) Experimental curve of the current decay process as the response time of the measurement system was 100 ms and 10 ms (inset). Reprinted with permission from [13], J. Zhou et al., *Appl. Phys. Lett.* 94, 191103 (**2009**). © 2009, American Institute of Physics.

RESEARCH ARTICLE

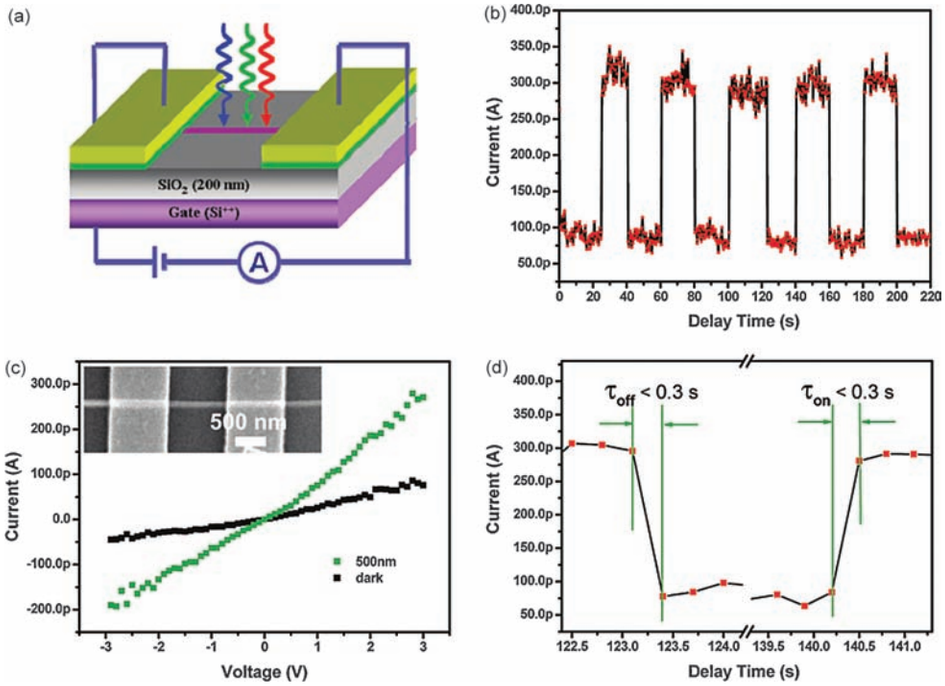

Fig. 9. (a) Schematic model of single In_2Se_3 NW photodetector. (b) *I–V* curve of the photodetector in dark and under 500 nm illumination. (c) Photoresponsive behaviour with pulsed incident 500 nm light. (d) Detailed view of the current rise and decay process, showing the fast response time below 1 s (the measurement limit of the setup is 0.3 s). Reprinted with permission from [2], T. Y. Zhai et al., *ACS Nano* 4, 1596 **(2010)**. © 2010, American Chemical Society.

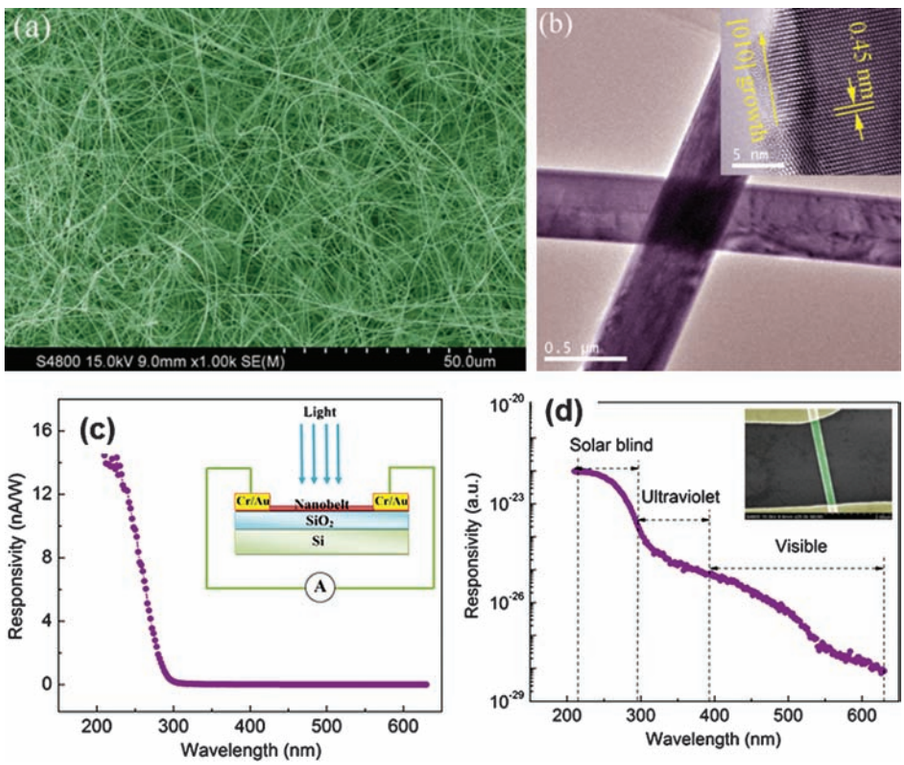

Fig. 10. (a) SEM image of the as-grown IGO nanobelts. (b) Low-magnification and HRTEM image of the single-crystalline IGO nanobelts. (c) Spectral response of IGO nanobelt photodetector with a cutoff wavelength < 290 nm. (d) Logarithmic plot of the spectral response showing the high wavelength selectivity. Inset is a typical SEM image of the device. Reprinted with permission from [14], L. Li et al., *Adv. Mater.* 22, 5145 **(2010)**. © 2010, Wiley-VCH Verlag GmbH & Co. KGaA.

RESEARCH ARTICLE

Fast response and reset time of 0.3 s (measurement limit of the experimental setup) were observed (Fig. 9(d)).[2] Similar fast photoresponse time was also observed in a series of photodetector reports using other materials.[2–4, 14, 19, 21, 25, 26, 34, 72, 73] Further efforts are still needed to fully understand why significant improvements were observed although similar device configurations with previous reports were adopted (e.g., single NW devices with symmetric electrodes and no surface decoration). However, the ultrafast photoresponse time down to the order of several ms or μs does represent dramatic improvements over previous studies.

3.3. High Wavelength Selectivity

High wavelength selectivity is an important characteristic for practical photodetection applications. Recently, remarkable processes have been made to fabricate NW photodetectors with high wavelength selectivity, especially those using wide bandgap semiconducting NWs. As a typical example, the photodetector performances of novel ternary indium germanate ($In_2Ge_2O_7$, IGO) nanobelts are shown in Figure 10.[14] IGO is a wide bandgap semiconductor (E_g = 4.43 eV) and has received increasing attention recently. Several unique 1D IGO nanostructures have been successfully synthesized, including microtubes, semi-nanotubes, NWs, nanobelts and hierarchical nanostructures.[14, 74–77] Representative SEM and transmission electron microscopy (TEM) images of the single-crystalline IGO nanobelts are shown in Figures 10(a and b), respectively.[14] Spectral response of single nanobelt photodetector (Fig. 10(d) inset) is shown in Figure 10(c).[14] The IGO device showed selective high response to deep-UV light (< 290 nm), with the highest responsivity at 230 nm.[14] The logarithmic plot of the spectral response gives a more detailed view of the responsivity throughout the wavelength range investigated (Fig. 10(d)).[14] It should be highlighted that the responsivity at 230 nm is 2–3 and 3–6 orders of magnitude higher than that in UV and visible light range, respectively.[14] This is consistent with the cut-off wavelength based on IGO bandgap of 4.43 eV (~280 nm) and was verified by the optical absorption spectrum (peaked at 244 nm).[14] Figure 10(d) also reveals the fact that the IGO nanobelt photodetector can detect light with sub-bandgap energy, although the responsivity is not as high as that in the deep-UV region. Detailed clarification of the sub-bandgap excitation in this rather complex ternary material still needs further efforts.

IGO nanobelt photodetector is an excellent example of wide bandgap semiconductor devices with high wavelength selectivity. Reports on the usage of other binary and ternary wide bandgap semiconductor NWs in photodetectors can also be found in recent literature.[4, 11, 13] Compared with binary semiconductors with bandgaps below 4 eV, novel ternary semiconductors (such as ZGO,[11, 72] IGO[14]) are advantageous for selective deep-UV detection. With further developments on the controllable synthesis of those wide bandgap ternary materials, they are expected to play crucial roles in the area of selective deep-UV detection.

Another group of ternary alloyed semiconductors with tunable compositions can also function as photodetectors with tunable wavelength selectivity. This type of materials was usually formed by alloying two binary semiconductors with similar chemical composition or crystal structure. For example, ternary $In_xGa_{1-x}N$ NWs with completely tunable chemical composition (from InN to GaN) were synthesized via a combinational CVD method.[78] As a result, the NW emission spectra can be continuously tuned from near-UV to near-infrared range.[78] This type of alloyed materials can also be used in photodetectors to efficiently control the wavelength selectivity.

Recently, Yoon et al. demonstrated the photodetecting properties of $Zn_xCd_{1-x}Se$ ($0 \leq x \leq 1$) NWs.[15] Structural characterizations of the alloyed NWs with different Zn concentrations are shown in Figure 11.[15] All the NWs were

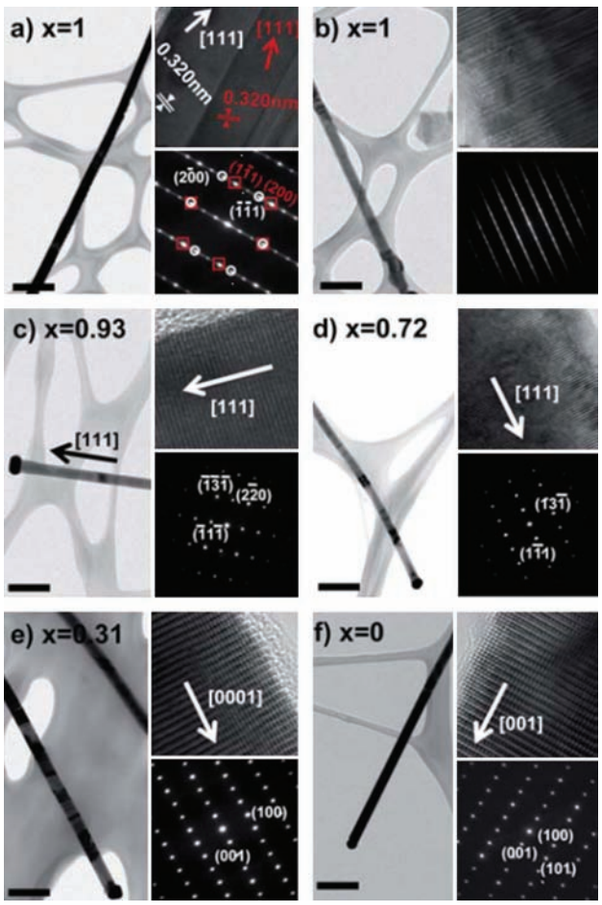

Fig. 11. TEM, HRTEM and SAED patterns of $Zn_xCd_{1-x}Se$ NWs with Zn concentrations of (a, b) 1; (c) 0.93; (d) 0.72; (e) 0.31 and (f) 0. Reprinted with permission from [15], Y. J. Yoon et al., *J. Mater. Chem.* 20, 2386 **(2010)**. © 2010, The Royal Society of Chemistry.

RESEARCH ARTICLE

single-crystalline except that stacking faults were observed in pure ZnSe NWs (Figs. 11(a–b)).[15] Crystal phase of the alloyed NWs transformed from cubic zinc blende (Zn-rich) to hexagonal wurtzite (Cd-rich) structure between 31% and 72% of Zn content.[15] Optical properties of the alloyed NWs are shown in Figure 12(a), which can be used to determine the bandgap variations (Fig. 12(b)).[15] The NW bandgap can be continuously tuned from 1.74 eV (CdSe) to 2.69 eV (ZnSe) with different Zn concentrations and this is highly desired for photodetector applications since the cut-off wavelengths are usually associated with the bandgaps. Spectral responses of the alloyed NWs with different compositions are shown in Figure 12(c).[15] As can be clearly viewed, higher responsivity was observed when the excitation wavelength was shorter than the cut-off wavelength. The longest cut-off wavelength was observed for CdSe with the smallest bandgap, which is consistent with theoretical expectations. The switching behaviours of 3 representative devices (ZnSe, $Zn_{0.31}Cd_{0.69}Se$ and CdSe) are shown in Figures 12(d–f), respectively.

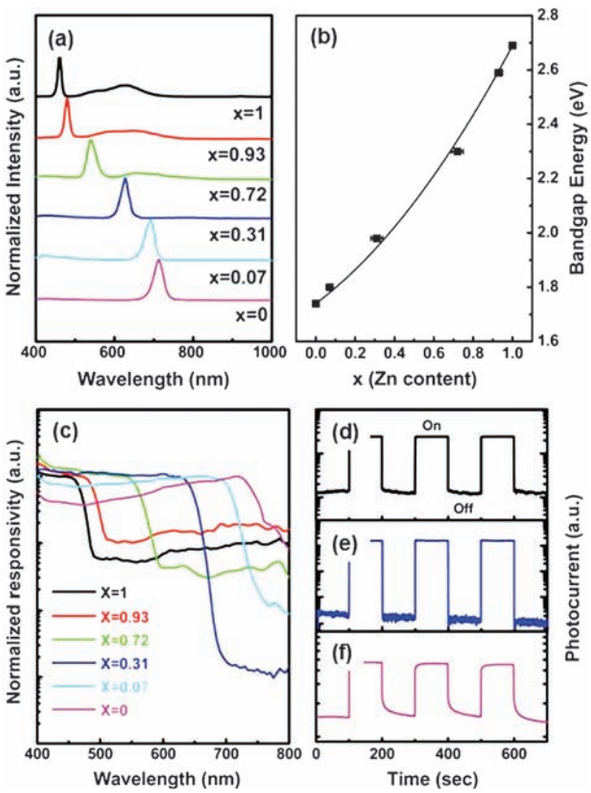

Fig. 12. (a) Room temperature PL emission from the alloyed NWs with different Zn concentration. (b) Plot of bandgap as a function of Zn content based on the PL emission. (c) Normalized spectral responses of alloyed NWs and the reversible switching behaviour of (d) ZnSe; (e) $Zn_{0.31}Cd_{0.69}Se$ and (f) CdSe devices. Reprinted with permission from [15], Y. J. Yoon et al., *J. Mater. Chem.* 20, 2386 (**2010**). © 2010, The Royal Society of Chemistry.

3.4. High Sensitivity

Sensitivity is an indispensable characteristic of NW photodetectors. High sensitivity is of great importance for the efficient detection of incident light with weak intensity. Recently, Wang et al. reported an novel approach to improve the sensitivity of ZnO NW photodetector by 5 orders of magnitude using polymer coating.[5] Typical photo-switching behaviours of the ZnO NW photodetectors with and without coatings are shown in Figure 13(a).[5] The native NW device without polymer coating showed a relatively low sensitivity (green line, ×10000). Devices coated with PS-co-Mac showed an improved sensitivity (black line, ×1000) and the best performance was achieved in those coated with PSS (red line).[5] However, PSS alone did not show any response to 280 nm UV light (blue line, ×500). The giant enhancement was attributed to the enhanced UV adsorption capabilities via surface funationalization.[5] In order to further explore the adsorption capabilities of different polymers, UV adsorption spectra of 4 different polymers were measured (Fig. 13(b)).[5] While PS-co-Mac (dark line), PNIPAM (blue line) and CMC (green line) only showed adsorption in the range of 190–200 nm, prominent adsorption peak was observed for PSS at ~260 nm, which is close to the wavelength of incident light (~280 nm).

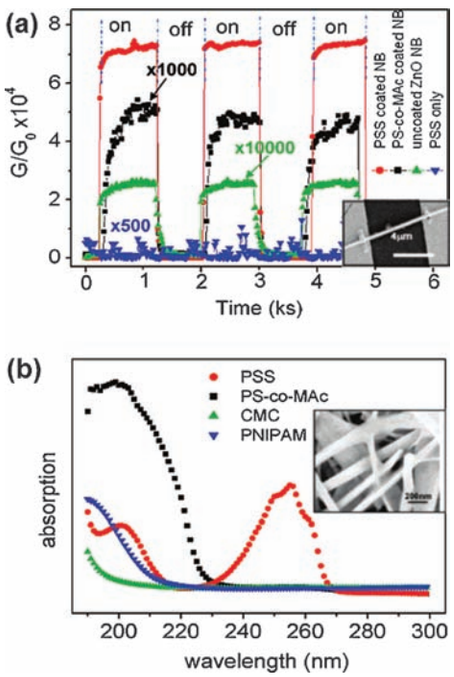

Fig. 13. (a) Normalized photoresponse curves of ZnO nanobelt devices: without coating (green line), PS-co-Mac coated (dark line), PSS coated (red line) and PSS only (blue line). (b) UV adsorption spectra of PSS (red line), PS-co-Mac (dark line), PNIPAM (blue line) and CMC (green line). Reprinted with permission from [5], C. S. Lao et al., *J. Am. Chem. Soc.* 129, 12096 (**2007**). © 2007, American Chemical Society.

The sensitivity enhancement via PS-co-Mac, PNIPAM and CMC coating can be understood via the trapping and delayed recombination of electrons and holes.[5] In brief, the surface coating will enhance the trapping of free electrons. Upon UV illumination, more holes would be attracted to the surface and result in a longer carrier lifetime and hence larger sensitivity.[5] However, this is not sufficient to explain the different enhancing capabilities between PSS and other polymers. PSS can adsorb or capture the incident phonons (∼280 nm) more effectively than other polymers (Fig. 13(b)).[5] Moreover, it is likely that the ground state energy of PSS lies between the bandgap of ZnO, acting as a "hopping" state to facilitate the excitation of electrons to ZnO conduction band. This PSS-assisted hopping process will greatly enhance the utilization of incident phonons and lead to giant sensitivity improvement.

Another efficient approach to improve the sensitivity of ZnO NW photodetector using piezo-phototronic effect was reported recently.[1] The ZnO NW devices were fabricated on a flexible PS substrate, with one free end bended using a 3D stage to apply a compressive or tensile strain.[1] Detailed device performances showing the sensitivity enhancement are shown in Figure 14.[1] Figure 14(a) is the dark *I–V* curves of the ZnO NW device under different stains and essentially no difference could be observed. Figures 14(b and c) are the *I–V* curves of the device under stain with illumination intensities of 2.2×10^{-5} W cm^{-2} and 3.3×10^{-2} W cm^{-2}, respectively.[1] The current difference is more prominent at negative bias with smaller illumination intensity, with the largest sensitivity improvement observed at compressive strain (−0.36%) (Fig. 14(b)).[1] The absolute current verses excitation intensity under different strains are plotted in Figure 14(b) to give a better comparative view of the performances. A sensitivity enhancement of 530% was achieved by applying a −0.36% compressive stain on the NW device illuminated with 4.9 pW incident light (372 nm).[1]

Minor Schottky barriers exist at the source and drain contacts for those ZnO NW photodetectors and the barrier height can be modified by the piezo-potential generated via applied stain. Under the specific device configurations, compressive strain would lead to a barrier height reduction at drain contact due to the positive piezopotential.[1] Consequently, the current level, i.e., responsivity would be enhanced compared that without strain. The enhancement is less prominent at high light intensity due to the screening effect[1] originating from the large amount of free electrons and holes. However, in dark conditions, the device resistance is dominated by the NW volume instead of the Schottky barrier. As a result, the effect of applied strain and hence piezo-potential is not as prominent as that with illumination.

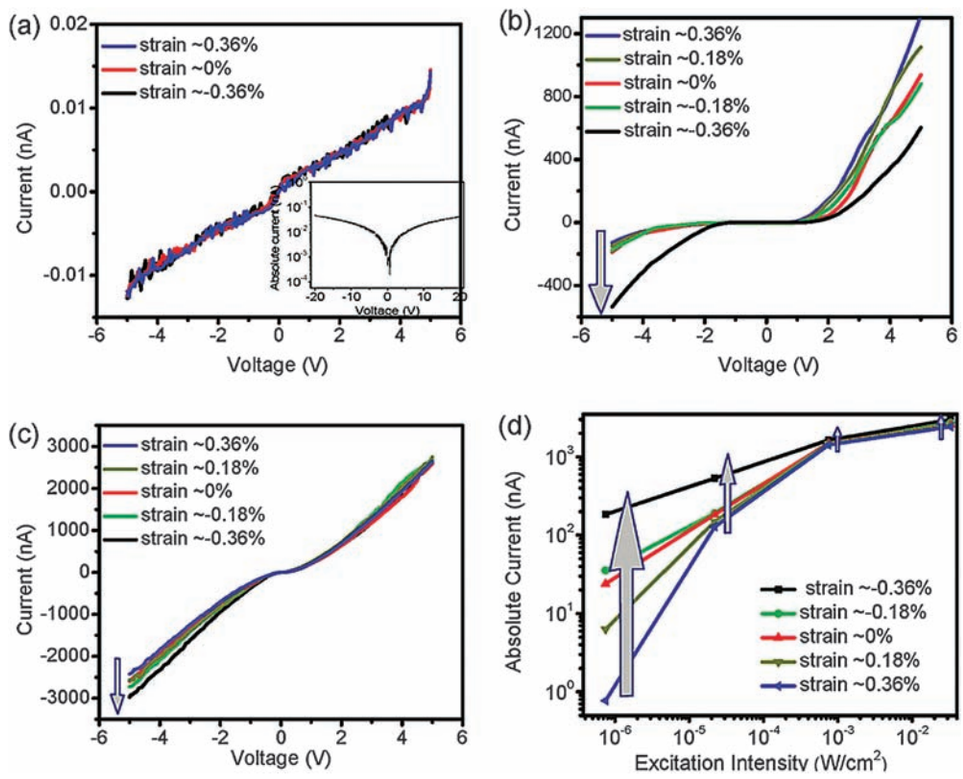

Fig. 14. (a) Dark *I–V* characteristics of ZnO NW device under stain. *I–V* curves of ZnO NW device under stain with illumination intensity of (b) 2.2×10^{-5} W cm^{-2} and (c) 3.3×10^{-2} W cm^{-2}. (d) Absolute photocurrent relative to excitation intensity under different stain. Reprinted with permission from [1], Q. Yang et al., *ACS Nano* 4, 6285 **(2010)**. © 2010, American Chemical Society.

RESEARCH ARTICLE

4. CONCLUSIONS AND OUTLOOK

In conclusion, we have presented the recent progresses in NW photodetector design and performances, including progresses in low-cost device fabrication, fast photoresponse time, high wavelength selectivity and high sensitivity. NW network devices, which only require facile and low-cost fabrication techniques, are considered as promising device configurations than single NW. Electronic and optoelectronic properties of network devices were characterized to be comparable or even superior than single NW devices. Facile and efficient assembly methods of NW networks have been demonstrated, which will further advance their applications. The network devices also showed fast photoresponse time, as have been shown in ZGO and Ge network devices. The enhanced photoresponse time was attributed to the unique NW–NW junction barrier in network devices, which is not available in single NW devices. Construction of Schottky-type photodetectors was also found to be an efficient method to enhance the photoresponse time. Ternary oxide nanostructures with wide bandgaps, such as IGO nanobelts, were demonstrated to be excellent candidates for selective deep-UV sensing. Tunable wavelength selectivity was achieved by forming alloyed $Zn_xCd_{1-x}Se$ NWs with different compositions and hence bandgaps. Sensitivity of ZnO NW photodetector was enhanced by 5 orders of magnitude via polymer functionalization, which was attributed to the polymer facilitated UV adsorption and electron transfer. Proper utilization of the unique piezo-electric properties of ZnO NWs also leads to significant enhancement of the NW photodetectors.

Apart from the progresses summarized in this review, other properties such as high stability and excellent performance consistency are also of crucial importance. Extensive efforts are still needed to fill the gap between lab research and commercial applications despite the significant progresses in the past years. Future research may mainly focus on:

(1) Improve NW alignment and network assembly methods to yield large scale uniform distribution, which is important for the fabrication of single NW and network device arrays with consistent performances.

(2) Improve the photodetector device configuration. Network devices and Schottky-type devices are significantly advances compared with conventional single-NW device with Ohmic contacts. However, more efforts are needed to further develop and optimize those methods. Alternatively, other innovative device configurations may be developed to yield high-performance devices.

(3) Enhance the controllability over the nanostructure design. Properties are closely related to the morphologies, compositions, doping or functionalization of the nanostructures. Thus it is of crucial importance to enhance the controllability to design novel and complex nanostructures with desired properties, which may potentially be used to enhance the photodetector performances.

(4) Integration of NW photodetectors to enable greater functionalities. Fabrication of medium or large scale integrated photodetector devices is certainly one of the future research directions. The integrated photodetector arrays may be used for more efficient light sensing and light imaging than individual devices. Moreover, photodetectors may be integrated with other devices on a single chip to enable greater functionalities, such as biological photometric sensing,[9] or self-powered nanophotonic circuits for chemical sensing.[79]

Acknowledgments: Chaoyi Yan thanks NTU for research scholarship. The authors also thank N. Singh, X. W. Lu and X. W. Yan for their support.

References and Notes

1. Q. Yang, X. Guo, W. H. Wang, Y. Zhang, S. Xu, D. H. Lien, and Z. L. Wang, *ACS Nano* 4, 6285 (**2010**).
2. T. Y. Zhai, X. S. Fang, M. Y. Liao, X. J. Xu, L. Li, B. D. Liu, Y. Koide, Y. Ma, J. N. A. Yao, Y. Bando, and D. Golberg, *ACS Nano* 4, 1596 (**2010**).
3. T. Y. Zhai, L. Li, X. Wang, X. S. Fang, Y. Bando, and D. Golberg, *Adv. Funct. Mater.* 20, 4233 (**2010**).
4. X. S. Fang, Y. Bando, M. Y. Liao, U. K. Gautam, C. Y. Zhi, B. Dierre, B. D. Liu, T. Y. Zhai, T. Sekiguchi, Y. Koide, and D. Golberg, *Adv. Mater.* 21, 2034 (**2009**).
5. C. S. Lao, M. C. Park, Q. Kuang, Y. L. Deng, A. K. Sood, D. L. Polla, and Z. L. Wang, *J. Am. Chem. Soc.* 129, 12096 (**2007**).
6. C. Soci, A. Zhang, B. Xiang, S. A. Dayeh, D. P. R. Aplin, J. Park, X. Y. Bao, Y. H. Lo, and D. Wang, *Nano Lett.* 7, 1003 (**2007**).
7. H. Kind, H. Q. Yan, B. Messer, M. Law, and P. D. Yang, *Adv. Mater.* 14, 158 (**2002**).
8. T. Y. Zhai, X. S. Fang, M. Y. Liao, X. J. Xu, H. B. Zeng, B. Yoshio, and D. Golberg, *Sensors* 9, 6504 (**2009**).
9. C. Soci, A. Zhang, X. Y. Bao, H. Kim, Y. Lo, and D. L. Wang, *J. Nanosci. Nanotech.* 10, 1430 (**2010**).
10. C. Y. Yan, N. Singh, H. Cai, C. L. Gan, and P. S. Lee, *ACS Appl. Mater. Interfaces* 2, 1794 (**2010**).
11. C. Y. Yan, N. Singh, and P. S. Lee, *Appl. Phys. Lett.* 96, 053108 (**2010**).
12. H. E. Unalan, Y. Zhang, P. Hiralal, S. Dalal, D. P. Chu, G. Eda, K. B. K. Teo, M. Chhowalla, W. I. Milne, and G. A. J. Amaratunga, *Appl. Phys. Lett.* 94, 163501 (**2009**).
13. J. Zhou, Y. D. Gu, Y. F. Hu, W. J. Mai, P. H. Yeh, G. Bao, A. K. Sood, D. L. Polla, and Z. L. Wang, *Appl. Phys. Lett.* 94, 191103 (**2009**).
14. L. Li, P. S. Lee, C. Y. Yan, T. Y. Zhai, X. S. Fang, M. Y. Liao, Y. Koide, Y. Bando, and D. Golberg, *Adv. Mater.* 22, 5145 (**2010**).
15. Y. J. Yoon, K. S. Park, J. H. Heo, J. G. Park, S. Nahm, and K. J. Choi, *J. Mater. Chem.* 20, 2386 (**2010**).
16. Y. Ahn, J. Dunning, and J. Park, *Nano Lett.* 5, 1367 (**2005**).
17. B. Gates, B. Mayers, B. Cattle, and Y. N. Xia, *Adv. Funct. Mater.* 12, 219 (**2002**).
18. Y. Wang, Z. Y. Tang, P. Podsiadlo, Y. Elkasabi, J. Lahann, and N. A. Kotov, *Adv. Mater.* 18, 518 (**2006**).
19. X. S. Fang, S. L. Xiong, T. Y. Zhai, Y. Bando, M. Y. Liao, U. K. Gautam, Y. Koide, X. Zhang, Y. T. Qian, and D. Golberg, *Adv. Mater.* 21, 5016 (**2009**).
20. Q. F. Meng, C. B. Jiang, and S. X. Mao, *Appl. Phys. Lett.* 94, 043111 (**2009**).

RESEARCH ARTICLE

21. L. Li, P. C. Wu, X. S. Fang, T. Y. Zhai, L. Dai, M. Y. Liao, Y. Koide, H. Q. Wang, Y. Bando, and D. Golberg, *Adv. Mater.* 22, 3161 **(2010)**.
22. Y. H. Yu, V. Protasenko, D. Jena, H. L. Xing, and M. Kuno, *Nano Lett.* 8, 1352 **(2008)**.
23. J. F. Wang, M. S. Gudiksen, X. F. Duan, Y. Cui, and C. M. Lieber, *Science* 293, 1455 **(2001)**.
24. M. Kang, J. S. Lee, S. K. Sim, H. Kim, B. Min, K. Cho, G. T. Kim, M. Y. Sung, S. Kim, and H. S. Han, *Jap. J. Appl. Phys.* 43, 6868 **(2004)**.
25. T. Y. Zhai, M. F. Ye, L. Li, X. S. Fang, M. Y. Liao, Y. F. Li, Y. Koide, Y. Bando, and D. Golberg, *Adv. Mater.* 22, 4530 **(2010)**.
26. L. Li, X. S. Fang, T. Y. Zhai, M. Y. Liao, U. K. Gautam, X. C. Wu, Y. Koide, Y. Bando, and D. Golberg, *Adv. Mater.* 22, 4151 **(2010)**.
27. D. S. Wang, C. H. Hao, W. Zheng, Q. Peng, T. H. Wang, Z. M. Liao, D. P. Yu, and Y. D. Li, *Adv. Mater.* 20, 2628 **(2008)**.
28. J. J. Wang, F. F. Cao, L. Jiang, Y. G. Guo, W. P. Hu, and L. J. Wan, *J. Am. Chem. Soc.* 131, 15602 **(2009)**.
29. H. F. Bao, C. M. Li, X. Q. Cui, Q. L. Song, H. B. Yang, and J. Guo, *Nanotechnology* 19, 335302 **(2008)**.
30. P. Wu, Y. Dai, Y. Ye, Y. Yin, and L. Dai, *J. Mater. Chem.* 21, 2563 **(2011)**.
31. Z. Q. Liu, D. H. Zhang, S. Han, C. Li, T. Tang, W. Jin, X. L. Liu, B. Lei, and C. W. Zhou, *Adv. Mater.* 15, 1754 **(2003)**.
32. D. Zhang, C. Li, S. Han, X. Liu, T. Tang, W. Jin, and C. Zhou, *Appl. Phys. A* 77, 163 **(2003)**.
33. X. Liu, C. Li, S. Han, J. Han, and C. W. Zhou, *Appl. Phys. Lett.* 82, 1950 **(2003)**.
34. T. Y. Zhai, H. M. Liu, H. Q. Li, X. S. Fang, M. Y. Liao, L. Li, H. S. Zhou, Y. Koide, Y. Bando, and D. Goberg, *Adv. Mater.* 22, 2547 **(2010)**.
35. P. Feng, J. Y. Zhang, Q. H. Li, and T. H. Wang, *Appl. Phys. Lett.* 88, 153107 **(2006)**.
36. L. C. Hsu, Y. P. Kuo, and Y. Y. Li, *Appl. Phys. Lett.* 94, 133108 **(2009)**.
37. L. Liao, B. Yan, Y. F. Hao, G. Z. Xing, J. P. Liu, B. C. Zhao, Z. X. Shen, T. Wu, L. Wang, J. T. L. Thong, C. M. Li, W. Huang, and T. Yu, *Appl. Phys. Lett.* 94, 113106 **(2009)**.
38. X. Q. Fu, C. Wang, P. Feng, and T. H. Wang, *Appl. Phys. Lett.* 91, 073104 **(2007)**.
39. Y. H. Chang, C. M. Liu, Y. C. Tseng, C. Chen, C. C. Chen, and H. E. Cheng, *Nanotechnology* 21, 225602 **(2010)**.
40. L. Li, Y. X. Zhang, X. S. Fang, T. Y. Zhai, M. Y. Liao, H. Q. Wang, G. H. Li, Y. Koide, Y. Bando, and D. Golberg, *Nanotechnology* 22, 165704 **(2011)**.
41. S. J. Chang, C. H. Hsiao, S. C. Hung, S. H. Chih, B. W. Lan, S. B. Wang, S. P. Chang, Y. C. Cheng, T. C. Li, and B. R. Huang, *J. Electrochem. Soc.* 157, K1 **(2010)**.
42. T. Y. Lui, J. A. Zapien, H. Tang, D. D. D. Ma, Y. K. Liu, C. S. Lee, S. T. Lee, S. L. Shi, and S. J. Xu, *Nanotechnology* 17, 5935 **(2006)**.
43. X. Y. Xue, Y. J. Chen, Q. H. Li, C. Wang, Y. G. Wang, and T. H. Wang, *Appl. Phys. Lett.* 88, 182102 **(2006)**.
44. P. Feng, J. Y. Zhang, Q. Wan, and T. H. Wang, *J. Appl. Phys.* 102, 074309 **(2007)**.
45. N. Garcia, J. Przeslawski, and M. Sharonov, *Surface Science* 407, L665 **(1998)**.
46. S. Miki, M. Fujiwara, M. Sasaki, B. Baek, A. J. Miller, R. H. Hadfield, S. W. Nam, and Z. Wang, *Appl. Phys. Lett.* 92, 061116 **(2008)**.
47. G. A. O'Brien, A. J. Quinn, D. A. Tanner, and G. Redmond, *Adv. Mater.* 18, 2379 **(2006)**.
48. X. J. Zhang, J. S. Jie, W. F. Zhang, C. Y. Zhang, L. B. Luo, Z. B. He, X. H. Zhang, W. J. Zhang, C. S. Lee, and S. T. Lee, *Adv. Mater.* 20, 2427 **(2008)**.
49. Y. J. Xing, G. Y. Jing, J. Xu, D. P. Yu, H. B. Liu, and Y. L. Li, *Appl. Phys. Lett.* 87, 263117 **(2005)**.
50. M. S. Hu, H. L. Chen, C. H. Shen, L. S. Hong, B. R. Huang, K. H. Chen, and L. C. Chen, *Nat. Mater.* 5, 102 **(2006)**.
51. C. H. Hsieh, L. J. Chou, G. R. Lin, Y. Bando, and D. Golberg, *Nano Lett.* 8, 3081 **(2008)**.
52. K. Sun, Y. Jing, N. Park, C. Li, Y. Bando, and D. L. Wang, *J. Am. Chem. Soc.* 132, 15465 **(2010)**.
53. G. Z. Shen, P. C. Chen, Y. Bando, D. Golberg, and C. W. Zhu, *Chem. Mater.* 20, 6779 **(2008)**.
54. S. P. Mondal and S. K. Ray, *Appl. Phys. Lett.* 94, 223119 **(2009)**.
55. C. H. Chen, S. J. Chang, S. P. Chang, M. J. Li, I. C. Chen, T. J. Hsueh, and C. L. Hsu, *Chem. Phys. Lett.* 476, 69 **(2009)**.
56. J. L. Sun, X. Zhao, and J. L. Zhu, *Nanotechnology* 19, 085703 **(2008)**.
57. Y. L. Chueh, C. H. Hsieh, M. T. Chang, L. J. Chou, C. S. Lao, J. H. Song, J. Y. Gan, and Z. L. Wang, *Adv. Mater.* 19, 143 **(2007)**.
58. M. Y. Lu, M. P. Lu, Y. A. Chung, M. J. Chen, Z. L. Wang, and L. J. Chen, *J. Phys. Chem. C* 113, 12878 **(2009)**.
59. X. Fan, X. M. Meng, X. H. Zhang, M. L. Zhang, J. S. Jie, W. J. Zhang, C. S. Lee, and S. T. Lee, *J. Phys. Chem. C* 113, 834 **(2009)**.
60. D. J. Pena, J. K. N. Mbindyo, A. J. Carado, T. E. Mallouk, C. D. Keating, B. Razavi, and T. S. Mayer, *J. Phys. Chem. B* 106, 7458 **(2002)**.
61. C. B. Winkelmann, I. Ionica, X. Chevalier, G. Royal, C. Bucher, and V. Bouchiat, *Nano Lett.* 7, 1454 **(2007)**.
62. Y. B. Guo, Q. X. Tang, H. B. Liu, Y. J. Zhang, Y. L. Li, W. P. Hu, S. Wang, and D. B. Zhu, *J. Am. Chem. Soc.* 130, 9198 **(2008)**.
63. D. C. Wei, Y. Q. Liu, L. C. Cao, H. L. Zhang, L. P. Huang, and G. Yu, *Chem. Mater.* 22, 288 **(2009)**.
64. K. Heo, E. Cho, J. E. Yang, M. H. Kim, M. Lee, B. Y. Lee, S. G. Kwon, M. S. Lee, M. H. Jo, H. J. Choi, T. Hyeon, and S. Hong, *Nano Lett.* 8, 4523 **(2008)**.
65. Z. Y. Fan, J. C. Ho, Z. A. Jacobson, R. Yerushalmi, R. L. Alley, H. Razavi, and A. Javey, *Nano Lett.* 8, 20 **(2008)**.
66. F. Fang, J. Futter, A. Markwitz, and J. Kennedy, *Nanotechnology* 20, 245502 **(2009)**.
67. Y. Liu, Z. Y. Zhang, H. L. Xu, L. H. Zhang, Z. X. Wang, W. L. Li, L. Ding, Y. F. Hu, M. Gao, Q. Li, and L. M. Peng, *J. Phys. Chem. C* 113, 16796 **(2009)**.
68. T. Hanrath and B. A. Korgel, *J. Phys. Chem. B* 109, 5518 **(2005)**.
69. G. Lubberts, B. C. Burkey, H. K. Bucher, and E. L. Wolf, *J. Appl. Phys.* 45, 2180 **(1974)**.
70. X. F. Duan, Y. Huang, Y. Cui, J. F. Wang, and C. M. Lieber, *Nature* 409, 66 **(2001)**.
71. Y. Cui and C. M. Lieber, *Science* 291, 851 **(2001)**.
72. C. Li, Y. Bando, M. Y. Liao, Y. Koide, and D. Golberg, *Appl. Phys. Lett.* 97, 161102 **(2010)**.
73. T. Y. Zhai, Y. Ma, L. A. Li, X. S. Fang, M. Y. Liao, Y. Koide, J. N. Yao, Y. Bando, and D. Golberg, *J. Mater. Chem.* 20, 6630 **(2010)**.
74. Y. Su, S. Li, L. Xu, Y. Q. Chen, Q. T. Zhou, B. Peng, S. Yin, X. Meng, X. M. Liang, and Y. Feng, *Nanotechnology* 17, 6007 **(2006)**.
75. J. H. Zhan, Y. Bando, J. Q. Hu, L. W. Yin, X. L. Yuan, T. Sekigitchi, and D. Golberg, *Angew. Chem., Int. Ed.* 45, 228 **(2006)**.
76. C. Y. Yan, T. Zhang, and P. S. Lee, *Cryst. Growth Des.* 8, 3144 **(2008)**.
77. C. Y. Yan, N. Singh, and P. S. Lee, *Cryst. Growth Des.* 9, 3697 **(2009)**.
78. T. Kuykendall, P. Ulrich, S. Aloni, and P. Yang, *Nat. Mater.* 6, 951 **(2007)**.
79. P. D. Yang, R. X. Yan, and M. Fardy, *Nano Lett.* 10, 1529 **(2010)**.

Received: xx Xxxx Xxxx. Accepted: xx Xxxx Xxxx.

RESEARCH ARTICLE